www.czasopisma.pan.pl PAN www.journals.pan.pl

ARCHIVES of FOUNDRY ENGINEERING

ISSN (2299-2944)
Volume 2020
Issue 2/2020

65 – 70

10.24425/afe.2020.131304

11/2

Published quarterly as the organ of the Foundry Commission of the Polish Academy of Sciences

The Crystallization of the AlSi9 Alloy Designed for the Alfin Processing of Ring Supports in Engine Pistons

J. Piątkowski [a, *], M. Czerepak [b]

[a] Silesian University of Technology, Faculty of Materials Science, Krasińskiego 8, 40-019 Katowice, Poland
[b] Federal-Mogul Gorzyce A Tenecco Group Company Pistons, 39-432 Gorzyce, Poland
* Corresponding author. E-mail address: jaroslaw.piatkowski@polsl.pl

Received 28.08.2019; accepted in revised form 22.01.2020

Abstract

This article presents a study of the crystallization and microstructure of the AlSi9 alloy (EN AC-AlSi9) used for the alfin processing of iron ring supports in castings of silumin pistons. Alfin processing in brief is based on submerging an iron casting in an Al-Si bath, maintaining it there for a defined time period, placing it in a chill mould casting machine and immersing it in the alloy. This technology is used for iron ring supports in the pistons of internal combustion engines, among others. Thermal analysis shows that when the AlSi9 alloy contains a minimal content of iron, nucleation and increase in the triple α(Al)+Fe+β(Si) eutectic containing the α-Al_8Fe_2Si phase takes place at the end of the crystallization of the double α(Al)+β(Si) eutectic. Due to the morphology of the "Chinese script" the α-Al_8Fe_2Si phase is beneficial and does not reduce the alloy's brittleness. After approx. 5 hours of alfin processing, the β-Al_5FeSi phase crystallizes as a component of the α+Al_5FeSi+β(Si) eutectic. Its disadvantageous morphology is "platelike" with sharp corners, and in a microsection of the surface, "needles" with pointed corners are visible, with increases the fragility of the AlSi9 alloys.

Keywords: Al-Si cast alloy, Alfin processing, Crystallization, Microstructure of Al-Si alloys

1. Introduction

Alfin processing in brief is based on submerging an iron casting in an liquid Al-Si alloy, maintaining it there for a defined time, and pouring liquid alloy [1÷3]. This technology is used for iron ring supports in the pistons of internal combustion engines, among others. Studies [4÷7] have concluded that the $Al_XFe_YSi_Z$ phases of various stoichiometric ratios are responsible for the durability of the bond between iron casting and Al alloy surfaces. Their morphology results from the conditions of crystallization and Fe content. Some of these phases solidify in the form of sharp edge plates which propagates microcracks, in turn causing the fragility and impermanence of the diffusion bond. It is therefore reasonable to study the solidification of the alloy and to determine the temperatures of crystallization of microstructure components.

2. Objectives and scope of the study

The objective of this study was to test the influence of varying Fe content on the crystallization process and the nature of the structure of the AlSi9 alloy for the alfin processing of iron ring supports located in combustion engine piston castings. This objective assumed the identification of characteristic temperatures of crystallization of the component phases and identification of the phases present in the studied alloy.

In order to realize these objectives, the study comprised, et al.:

- analysis of the solidification process of the alloy for alfin processing using thermal and derivative analysis,
- designation of characteristic temperatures of solidification of the alloy for alfin processing,
- study of the microstructure of the alloy for alfin processing.

3. Method and material of the study

The material for study was AlSi9 alloy, which is owned by Federal-Mogul. Samples were taken from the alloy during the alfin processing (temperature 780°C over 20 s.) of ring supports at the following points in time:

– before initiation of alfin processing – i.e. alloy designated as **S0**,
– 5 hours into alfin processing – i.e. **S5** alloy,
– 10 hours into alfin processing – i.e. **S10** alloy,
– after 15 hours of alfin processing – i.e. 'scrapped' **S15** alloy.

Initial studies indicated that after approx. 15 hours of alfin processing, AS9 alloy attained a critical value of 3.5% Fe, which made it production scrap, withdrawn from the technological process (based on the Technical Specifications Pistons TS1E-022-002 by Federal-Mogul Tenecco Group Company).

Samples were melted in an electric resistance furnace crucible of PT12/100-PCH type and after attaining a temperature of approx. 780°C they were poured into a the QC-4080 Heraeus Electro-Nite ceramic sampler of 130 cm^3 in volume. The crystallization temperature (t) and its first derivative after the time (dt/dτ) was registered with the use of the NiCr-NiAl thermoelement (type K) located in the axis of the sampler. Thermal and derivative analysis was conducted with the NT3-8K Crystaldigraph. Maximum on the derivative curve (dt/dτ) means phase or component of the structure is released. Thermal analysis was repeated three times. Samples for microstructure testing were removed from the temperature measurement area of the sample.

Metallographic studies were conducted on the MeF-2 Reichert microscope. An X-ray microanalysis was conducted on the Hitachi S-4200 scanning microscope coupled with the EDS Voyager X-ray. Analysis of the chemical composition in micro-areas was conducted with energy-dispersive X-ray microanalysis using the Thermo Noran detector. X-ray imaging was conducted using a the Philips X`Pert diffractometer, using a the $\lambda Cu_{K\alpha}$ – 1.54178 Å lamp, powered by 30 mA and 40 kV current. Registration was performed using a step-scanning method with a 0.04° step and 10 s time periods in the range of the angle 2θ from 20° to 140°.

4. Research results

Results of the chemical composition of the alloy for alfin processing of ring supports are presented in Table 1.

Table 1.
Results of the study of the chemical composition of the AlSi9 alloy (Al – remaining component) [1]

Chemical composition, wt. %								
Si	Fe	Mg	Cu	Mn	Ni	Cr	Zn	Other[2]
before starting the alfin processing– **S0** alloy								
7.949	**0.356**	0.006	0.021	0.025	0.041	0.005	0.041	0.058
after 5 hours of alfin processing –**S5** alloy								
8.080	**1.543**	0.005	0.138	0.043	0.280	0.026	0.035	0.060
after 10 hours of alfin processing –**S10** alloy								
8.170	**2.421**	0.004	0.268	0.082	0.510	0.061	0.040	0.078
after 15 hours of alfin processing –**S15** alloy								
8.114	**3.650**	0.005	0.330	0.110	0.845	0.084	0.040	0.092

[1] – average results from 6 measurements, after elimination of two extreme results,
[2] – the sum of the remaining elements and contamination in AlSi9 alloy.

4.1. Results of thermal analysis of AlSi9 alloy

The solidification for the alfin process is shown in Figure 1. The crystallization tests were performed in similar ambient conditions and applying the same smoothing coefficients.

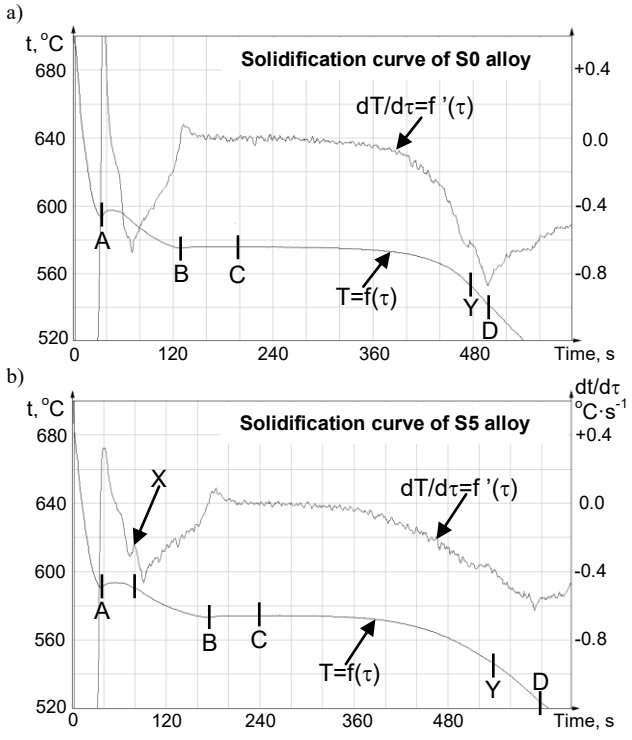

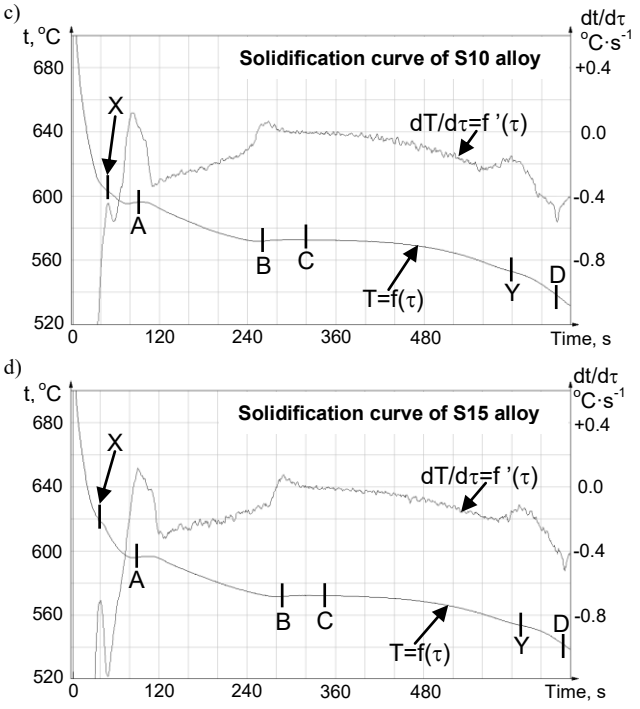

Fig. 1. Thermal curve and its derivative during alfin processing designated as: a) S0; b) S5; c) S10 and d) S15 alloy

Symbols and points in Figure 1 symbolize:

t=f(τ) – curve of temperature change in time τ,
dt/dτ=f'(τ) – first derivative of temperature change in time τ,
point A – $T_{\alpha(Al)}$ temperature of dendritic solidification α, °C,
point B – $T_{Emin(\alpha+\beta)}$ – min. eutectic point α(Al)+β(Si), °C,
point C – $T_{E(\alpha+\beta)}$ – avg eutectic point α(Al)+β(Si), °C,
point D – $T_{sol.}$ – end point alloy solidification temperature, °C,
point X – $T_{E(Fe)}$ – solidification temperature of the intermetallic iron phases, °C,
point Y – $T_{E'(Fe)}$ – solidification temperature of the low-melting intermetallic iron phases, °C.

The table with average values for the crystallization temperature for AlSi9 alloy (rounded to their full values) for varying iron content from the thermal analysis is presented in Table 1.

Table 2.
Solidification temperatures from thermal analysis curves (Fig. 1)

Alloy name	Characteristic temperatures, °C points on thermal analysis curves - from Figure 1.					
	X	A	B	C	Y	D
	$T_{E(Fe)}$	$T_{\alpha(Al)}$	$T_{Emin(\alpha+\beta)}$	$T_{E(\alpha+\beta)}$	$T_{E'(Fe)}$	$T_{sol.}$
S0	–	595	575	578	555	546
S5	590	592	576	577	547	528
S10	608	594	575	577	551	540
S15	620	595	573	576	556	538

4.2. Results of the microstructure of AlSi9 alloy

Sample microstructures for AlSi9 alloy before and during alfin processing are presented in Figure 2.

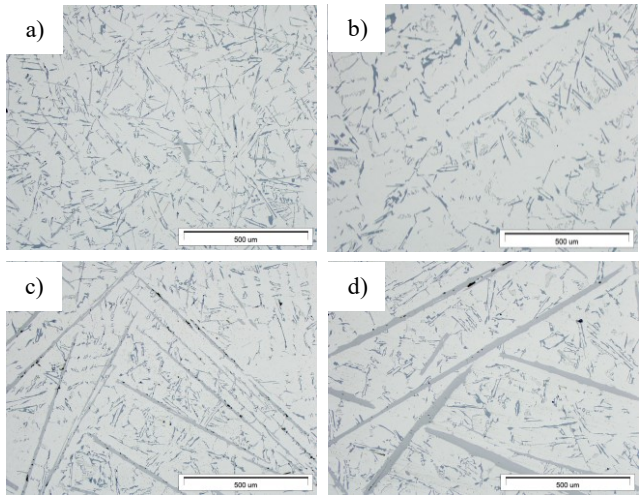

Fig. 2. The microstructure (LM) of the: a) S0; b) S5; c) S10; d) S15 alloy

SEM microstructure of the AlSi9 alloy is shown in Figure 3.

Example EDS image with weight and atomic shares for S10 alloy are presented in Figure 4.

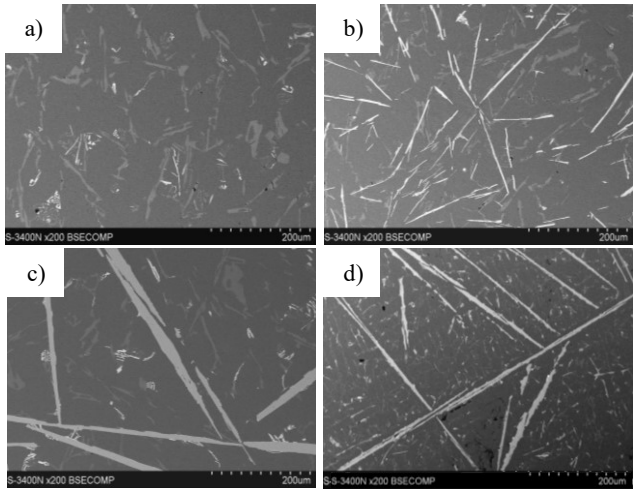

Fig. 3. The microstructure (SEM) of the: a) S0; b) S5; c) S10; d) S15 alloy

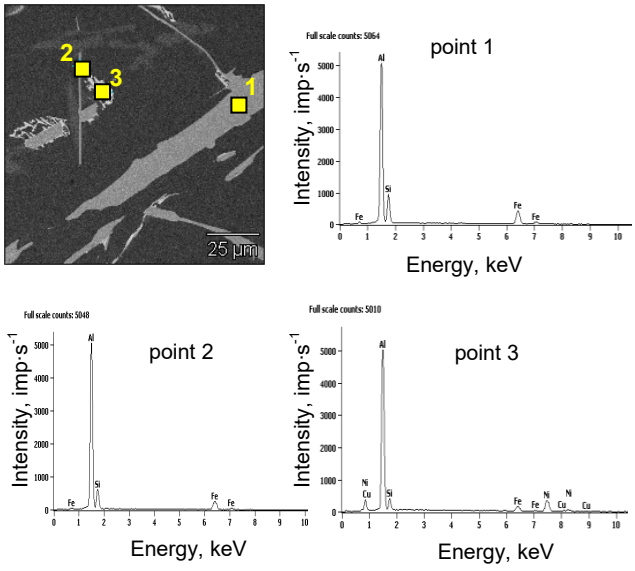

Weight %

alloy	*Cu*	*Al*	*Si*	*Fe*	*Ni*
S10		51.6	13.4	35.0	
S10		59.6	12.5	28.0	
S10	3.8	47.8	4.3	9.3	34.8

Atom %

alloy	*Cu*	*Al*	*Si*	*Fe*	*Ni*
S10		63.4	15.9	20.8	
S10		70.0	14.1	15.9	
S10	2.2	64.6	5.5	6.1	21.6

Fig. 4. EDS image of element concentration by weight and atomic share in microareas of S10 alloy

X-ray diffraction pattern of the S5 and S15 alloys are presented in Figure 5.

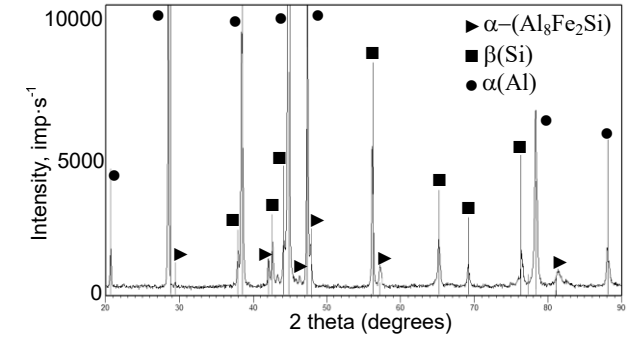

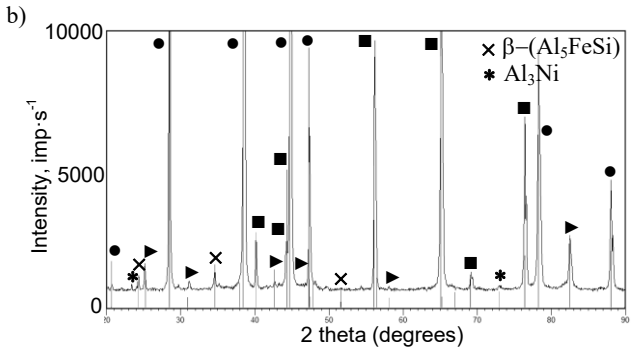

Fig. 5. X-ray diffraction pattern of the a) S0 and b) S15 alloys

5. Research results and their discussion

Thermal and derivative analysis shows that crystallization of AlSi9 alloy start of the alfin processing ensues in a traditional manner for silumins of near-eutectic composition. At first, dendritic crystallization of the solid solution α(Al) occurs at a temperature of 595°C. This is compatible with the Al-Si phase diagram. With the end of their solidification, double α(Al)+β(Si) eutectic nucleation and crystallization takes place at a temperature of approx. 578°C, which precedes a small degree of undercooling to $T_{Emin.(\alpha+\beta)}$=575°C. Crystallization of α(Al)+Fe+β(Si) eutectic takes place at a range of approx. 550÷560°C (Y area); this includes the intermetallic α-Al_8Fe_2Si phase (Figure 5a). Because none significant amounts of other additional components are present in S0 alloy, the crystallization of this eutectic lasts to the attainment of the temperature 546°C, which ends the process of the crystallization and solidification of the alloy.

After five hours of alfin processing, an additional exothermic effect $T_{E(Fe)}$=590°C (X point) was determined on the crystallization curve (Figure 1b) after dendritic nucleation and crystallization of the Al solution. Structural tests (Figure 5b) indicate that this is most probably the intermetallic β-Al_5FeSi phase. The further course of dendritic crystallization of the α(Al) S5 alloy is similar to the S0 alloy. After dendritic crystallization of the solid solution α(Al) and the crystallization of the double α(Al)+β(Si) eutectic and the triple α(Al)+Fe+β(Si) eutectic, which contains the intermetallic α-Al_8Fe_2Si phase, the end of crystallization takes place at temperature $T_{sol.}$, at which it should be noted that its value underwent a reduction of approx. 18°C. The curve of the AlSi9 alloy solidification after 10 hours of alfin processing indicates that the intermetallic β-Al_5FeSi phase crystallizes first at a temperature of 608°C. The increase of the temperature $T_{E(Fe)}$ is probably related to the increase of the iron content from 1.54% (for S5 alloy) to 2.42% (for S10 alloy), and to be precise, to the increase in the count of the β-Al_5FeSi phase. The range of α(Al)+Fe+β(Si) eutectic crystallization remains unchanged [7].

Thermal curve for the alloy after 15 hours of alfin processing indicates that the crystallization temperature of the intermetallic Al_5FeSi phase is still higher, approx. 620°C (X point Figure 1d), which is related to even greater content of iron in the alloy (3.65 wt %). Therefore it is clearly visible that the increase in the share of iron content in the AlSi9 alloy causes an increase in the

crystallization temperature of the disadvantageous β-Al_5FeSi phase, with no change in the range of solidification of the triple α(Al)+Fe+β(Si) eutectic, which contains the intermetallic α-Al_8Fe_2Si phase. These dependencies are presented in Figure 6.

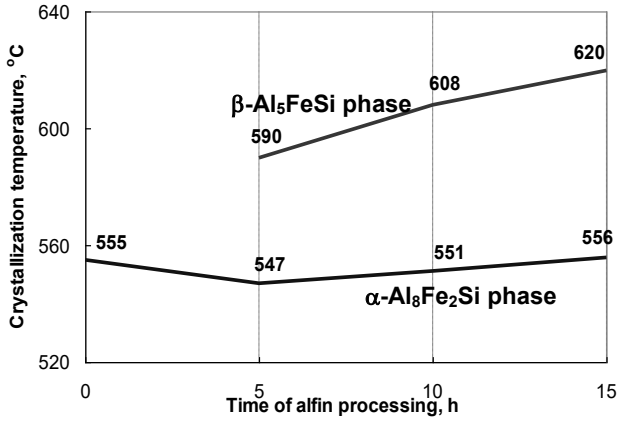

Fig. 6. The relationship between iron content and the crystallization temperature of the Al_XFe_YSi phases

On the basis of microscopic tests it may be stated that before alfin processing of AlSi9 alloy, classical component structures are present i.e.: a matrix comprised of the dendrites of the solid solution α(Al), a separation of the double α(Al)+β(Si) eutectic and few separations of the intermetallic α-Al_8Fe_2Si phases (Chinese script- Figures 7 and 8). After 5 hours of alfin processing and the increase in the iron content to 1.54 wt. %, an increase in the share of the α-Al_8Fe_2Si phase appears along with few separations of the β-Al_5FeSi phase of a length of about 100÷200 μm [6]. Continued alfin processing (10 hours) and related increase in the content to approx. 2.42 wt. % Fe causes an even greater share of the β-Al_5FeSi phase. Their surface areas significantly increase, and their length even reaches approx. 2 mm [6].

Extension of time to 15 hours of alfin processing and increase in the share of iron to approx. 3.65 wt. % no longer causes the extension of the ”needles” of the β-Al_5FeSi phase; it only causes an increase in their width [6]. Their morphology becomes very disadvantageous. These are plate-shaped separations with sharp edges; at the surface of the metallographic specimen they are visible as “needle” separations with pointed corners. As they are very hard and brittle, they have a disadvantageous influence on the performance characteristics of the alloys. They also are the first locations for the formation of porosity, because they cause the reduction of the interdendritic capacity, blocking the free flow of the liquid phase in the casting [5]. In the case of chill moulds, the advancing crystallization front doesn’t ”keep up” with the filling of these spaces with liquid metal, causing the formation of pores and microshrinkage porosity in the proximity of the needles of the β-Al_5FeSi phase – as shown in Figure 7.

Figure 8 shows the microstructure of the S15 alloy after deep etching with visible precipitation of the α-Al_8Fe_2Si phases in the morphology of ”Chinese script” and β-Al_5FeSi phases in the morphology of platelets.

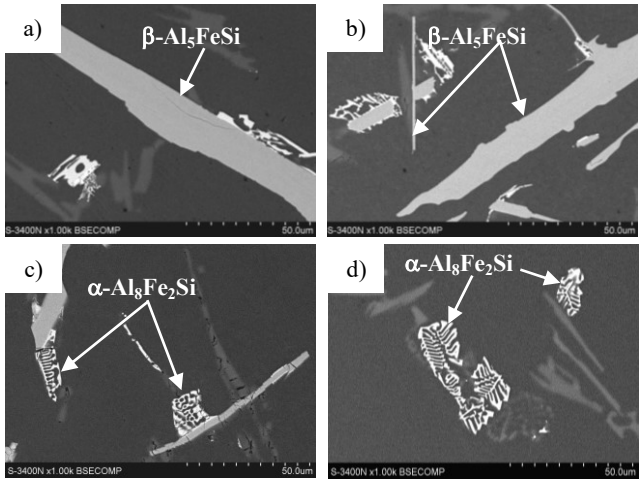

Fig. 7. The intermetallic: a-b) β-Al_5FeSi and c-d) α-Al_8Fe_2Si phases in the AlSi9 alloy after 15 hours of alfin processing

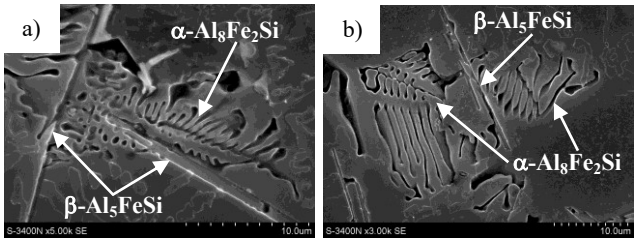

Fig. 8. a-b) the microstructure of the S15 cast alloy after 15 hours alfin processing after deep etching with visible precipitation of α-Al_8Fe_2Si and β-Al_5FeSi phases

6. Conclusions

The following conclusions have been formulated on the basis of this study:

1. Analysis of the chemical composition of the AlSi9 alloy showed that during the alfin processing iron increases from 0.356 wt.% (before starting the alfin process) to 3.65 wt.% (after 15 hours of alfin process). This is on average about 0.24 wt. % Fe every hour.
2. In the AlSi9 alloy, the α-Al_8Fe_2Si intermetallic phase has been identified, which looks like ”chinese script”.
3. From 5 to 15 hours of alfin processing of ring inserts for engine piston castings in the AlSi9 alloy, the β-Al_5FeSi phase was identified. This phase has a morphology of ”thin plates” and ”long needles” on the surface of the specimen.
4. It can be assumed that the size and morphology of the β-Al_5FeSi phase impedes the mechanical processing of the engine piston castings and causing local cracking in the ring-piston interface.

References

[1] Acar, A.F., Ozturk, F. & Bayrak, M. (2010). Effect of variations in alloy content and machining parameters on the strength of the intermetallic bonding between a diesel piston and a ring carrier. *Materials and Technology.* 44(6), 391-395. DOI: 621.436 UDK.

[2] Manasijevic, S., Dolic, N., Djurdjevic, M., Misic, N. & Davitkov, N. (2015). The intermetallic bonding between a ring carrier and aluminum piston alloy. *Revista de Metalurgia.* 51(3), 1-7. DOI: 10.3989/revmetalm.048.

[3] Manasijevic, S. & Radisa, R. (2015). Al-Fin Bond in Aluminum Piston Alloy & Austenitic Cast Iron Insert. *International Journal of Metalcasting.* 9(4), 27-32. DOI: 10.1007/BF03356037.

[4] Szajnar, J., Wróbel, T., Dulska, A. (2017). Manufacturing methods of alloy layers on casting surfaces. *Journal of Casting and Materials Engineering.* 1(1), 2-6. DOI: ORG/ 10.7494/jcme.2017.1.1.2.

[5] Xinjin, Cao & Campbell, J. (2006). Morphology of β-Al5FeSi phase in Al-Si cast alloy. *Material Transactions* 47, 1303-1312. DOI: 10.2320/matertrans.47.1303.

[6] Report from assignment no 4500314245 commissioned by the Federal-Mogul Gorzyce Tenecco Company. (unpublished materials, in Polish).

[7] Yoshiaki Osawa, Susumu Takamori, Takashi Kimura, Kazumi Minagawa and Hideki Kakisawa (2007) Morphology of intermetallic compounds in Al-Si-Fe alloy and its control by ultrasonic vibration. *Materials Transactions.* 48(9), 2467-2475. DOI: 102320/matertrans.F-MRA2007874.